IEEE Access
Multidisciplinary | Rapid Review | Open Access Journal

Received January 11, 2022, accepted February 19, 2022, date of publication March 3, 2022, date of current version March 11, 2022.

Digital Object Identifier 10.1109/ACCESS.2022.3156604

Error Control on Mobile Station Sides in Collaborative Multiple-Input Multiple-Output Systems

HOKUTO TAROMARU[1], (Student Member, IEEE), HIDEKAZU MURATA[1], (Member, IEEE), TOSHIRO NAKAHIRA[2], DAISUKE MURAYAMA[2], (Member, IEEE), AND TAKATSUNE MORIYAMA[2]

[1]Graduate School of Informatics, Kyoto University, Kyoto 606-8501, Japan
[2]NTT Access Network Service Systems Laboratories, NTT Corporation, Yokosuka 239-0847, Japan

Corresponding author: Hidekazu Murata (murata@i.kyoto-u.ac.jp)

ABSTRACT Collaboration between mobile stations (MSs) may lead to a new form of wireless communication. Collaboration on MS sides considerably improves signal detection performance, especially for multiple-input multiple-output (MIMO) transmission systems. In this study, a novel detector collaboration system is proposed to reduce the traffic volume on inter-MS collaboration links. Multiple MSs in the immediate vicinity are used to collaboratively decode the MIMO signals received from a base station. Furthermore, we consider a distributed detection system, in which multiple detection MSs decode the MIMO signals independently. Multiple decision results are exploited to improve the error performance. Residual interference coefficients were used to finalize the decision results. The error ratio performance and the traffic volume over collaboration wireless links were compared with those of two combining schemes through computer simulations and field experiments. The results revealed that the proposed error control scheme on mobile station sides offers a better tradeoff between the error performance and the traffic volume on the collaboration wireless links.

INDEX TERMS Cooperative communications, collaborative communications, HARQ, distributed MIMO.

I. INTRODUCTION

Collaboration on a mobile station (MS) sides can considerably improve signal detection performance [1]–[4]. Especially, in multiple-input multiple-output (MIMO) transmission systems, the increased number of antennas on the MS side can be used to enhance the channel capacity [5] and detection performance [6], [7]. In collaborative MIMO detection systems, collaborative MS groups that consist of MSs in the immediate vicinity are formed to collaboratively decode the MIMO signals transmitted from a base station (BS).

We focus on physical-layer collaboration to improve transmission performance from the BS to the collaborative MS group. An MS in the collaborative MS group forwards the signal waveform received from the BS to an MS in charge of detection (detection MS). In this scenario, the number of receive antennas on the MS side is considerably higher than that of a single MS. Therefore, the channel capacity and detection performance [7], [8] can be enhanced.

Wireless links connecting MSs for collaboration are crucial for this collaborative detection system. Furthermore, the wireless links should be high speed and low latency to provide a physical-layer collaboration of MSs in the group. Thus, a higher-frequency band transmission technology should be preferred (e.g. 5G NR). Increasing the number of MSs in the collaborative MS group offers a superior detection performance [9]. However, more collaboration traffic is incurred in the collaborative wireless links because of the increased number of forwarded waveforms.

The authors in [10] focused on the broadcast of wireless media and proposed distributed detection schemes to improve detection performance with the same number of forwarded waveforms. In these schemes, a neighboring MS (second-detection MS) overhears the forwarded waveforms and then independently decodes the MIMO signals transmitted from the BS. If a unique set of signals is used in each detection MS, the decision results differ. Therefore, MIMO detection performance can be improved by appropriately utilizing the

The associate editor coordinating the review of this manuscript and approving it for publication was Mauro Fadda.

results of multiple detection MSs. Notably, overhearing does not require additional traffic. The traffic volume of the decision result exchange is generally lower than that of waveform forwarding.

In the distributed detection scheme [10], detection MSs independently decode the MIMO signal streams from the BS. Each detection MS uses the waveforms forwarded by the helper MSs as well as its own received signal from the BS. Thus, distinct sets of MIMO received signals are used in each detection MS, delivering different decision results. This difference can be exploited to improve detection performance. In [10], every detected bit sequence (DBS) was gathered through collaboration links to determine the most reliable DBS for each stream. This scheme always imposes additional traffic on the collaboration wireless links to gather the decision results from other detection MSs.

We improve our prior approach [10] and propose an error-control scheme with reduced collaboration traffic on the MS side. In the proposed scheme, multiple detection MSs are used to enhance detection performance, similar to the approach in [10], while keeping the collaboration traffic volume as small as possible by using on-demand DBS exchange based on reliability information [11]. For simplicity, we assume that one of the detection MSs is a target information sink. The proposed scheme operates as follows: First, a target MS checks the reliabilities of its own DBSs. Provided its own DBS of a stream is of low reliability, the target MS requests a DBS of the stream along with its reliability information from another detection MS. This process is repeated until the DBSs of all detection MSs are examined or the reliability satisfies the criterion. In this study, the error performance is investigated through extensive computer simulations and experimental evaluations.

The major contributions of this paper are as follows:

1) An on-demand reliability-based MS-side error-control scheme that utilizes multiple detection MSs is described.
2) The frame error ratio (FER) performance of the proposed scheme is compared with those of the majority combining (MC) scheme and log-likelihood ratio (LLR) combining schemes.
3) The FER performance comparison is performed assuming correlated fading channels.
4) The performance advantage of the proposed scheme is demonstrated using the recorded signals of the measurement campaign.

This study expanded the results of [11]. The points 2), 3), and 4) present new results. The remainder of this paper is organized as follows. The system model of the collaborative MIMO systems is described in Section II. Section III introduces an iterative equalization and detection scheme in the frequency domain. The proposed reliability-based MS-side error-control scheme is described in Section IV. Section V presents the computer simulation results. The experimental setup and experimental results are discussed in Section VI. Finally, the conclusions are presented in Section VII.

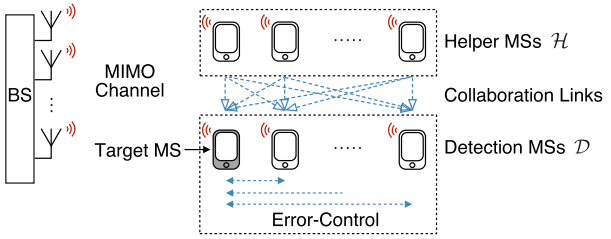

FIGURE 1. Distributed detection system with on-demand DBS requests. Helper MSs forward the received signals from the BS to the detection MSs. The target MS requests another decision result from other detection MSs, if necessary.

II. SYSTEM MODEL

A system model of an MS-side error-control scheme in a distributed MIMO detection system is displayed in Fig. 1. In this system, M independent MIMO signal streams are transmitted from the BS to a collaborative MS group ($\mathcal{H} \cup \mathcal{D}$). The MSs in this group are equipped with a single antenna each. In the collaborative MS group, helper MSs ($\mathcal{H}, h = |\mathcal{H}|$) forward the signals to detection MSs ($\mathcal{D}$, $d = |\mathcal{D}|$) through collaboration wireless links after receiving the signals from the BS. A high-speed low-latency wireless communication technique operating in high-frequency bands is suited for the proposed technique.

In the collaborative MS group, the detection MSs receive the forwarded signals as well as the signal transmitted from the BS. Using these signals, each detection MS independently decoded the MIMO signal streams from the BS. The decision results of each detection MS may differ from those of the other detection MSs because each detection MS received signal for detection. For simplicity, we assumed that the M signal streams are transmitted to a single-detection MS (target MS). Thus, the target MS is an information sink, and d decision results are available in the collaborative MS group. To take advantage of the multiple decision results, the reliability of the decision results is employed as a result selection metric in [10]. We proposed an error-control method on the MS side to reduce the traffic volume over collaboration wireless links. In the proposed technique, the target MS requests results from another detection MS when the target MS finds that: the reliability of the current results is not satisfactory.

III. DETECTION SCHEME

A. ITERATIVE MIMO DETECTION IN THE FREQUENCY DOMAIN

The frequency-domain (FD) iterative MIMO detection scheme is illustrated in Fig. 2. This detection scheme iteratively decodes single-carrier MIMO signals using FD soft cancellation followed by a minimum mean-squared error (MMSE) filter [12], [13]. In this detector, the $L = h + 1$ received signals available at the detection MSs, namely the own received signals and the h signals forwarded from the helper MSs, are used. The iterative detection scheme includes

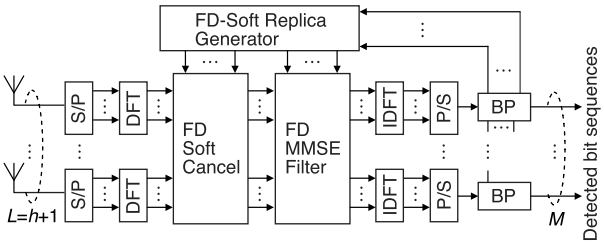

FIGURE 2. Frequency-domain iterative MIMO detection scheme.

three processes: i) Interference (other streams) cancellation using soft replicas (after the first iteration), ii) MMSE-based MIMO signal separation and equalization, and iii) soft decoding with belief propagation (BP).

The received kth ($1 \leq k \leq K$) symbol is denoted by $y_l(k)$ ($1 \leq l \leq L$). Next, the received signal vector $\boldsymbol{y}(k) = [y_1(k), y_2(k), \ldots, y_L(k)]^{\mathrm{T}} \in \mathbb{C}^{L\times 1}$ is expressed by the following,

$$\boldsymbol{y}(k) = \boldsymbol{H}\boldsymbol{x}(k) + \boldsymbol{n}(k), \tag{1}$$

where the superscript $(.)^{\mathrm{T}}$ denotes the transpose operation, $\boldsymbol{H} \in \mathbb{C}^{L\times M}$ is a channel matrix in which the channel variations are negligible over the K-symbol period, and $\boldsymbol{x}(k) \in \mathbb{C}^{M\times 1}$ and $\boldsymbol{n}(k) \in \mathbb{C}^{L\times 1}$ are the transmitted symbol vector and additive white Gaussian noise vector, respectively. The FD MIMO received signal vector $\boldsymbol{y}(f) \in \mathbb{C}^{L\times 1}$ is equalized in the MMSE filters $\boldsymbol{w}_m(f) \in \mathbb{C}^{L\times 1}$ as follows:

$$\tilde{x}_m(f) = \boldsymbol{w}_m^{\mathrm{H}}(f)\boldsymbol{y}(f), \tag{2}$$

$$\boldsymbol{w}_m(f) = \left(\sum_i \boldsymbol{h}_i(f)\boldsymbol{h}_i^{\mathrm{H}}(f) + \sigma^2\mathbf{I}_L\right)^{-1} \boldsymbol{h}_m(f), \tag{3}$$

where superscript $(.)^{\mathrm{H}}$ denotes the Hermitian transpose and $\boldsymbol{h}_i(f) \in \mathbb{C}^{L\times 1}$ represents the ith column of the FD channel matrix $\boldsymbol{H}(f)$. σ^2 is the noise variance, and $\mathbf{I}_L$ is the $L \times L$ identity matrix.

The MMSE filter output signals $\tilde{\boldsymbol{x}}(k) \in \mathbb{C}^{M\times 1}$ in the time domain (TD) are fed into the BP decoder. In the BP decoder, LLRs $L(c_{m,k,i})$ are calculated iteratively (inner iteration), where $c_{m,k,i}$ denotes the ith bit of the kth symbol in the mth signal stream.

Provided that quadrature phase-shift keying (QPSK) modulation is used, soft-decision symbols $\hat{\boldsymbol{x}}(k) = [\hat{x}_1(k), \hat{x}_2(k), \ldots, \hat{x}_M(k)]^{\mathrm{T}} \in \mathbb{C}^{M\times 1}$ are generated in an FD soft replica generator as follows:

$$\hat{x}_m(k) = \frac{1}{\sqrt{2}}\tanh\left(L(c_{m,k,1})/2\right) + \frac{1}{\sqrt{2}}\tanh\left(L(c_{m,k,2})/2\right)\sqrt{-1}. \tag{4}$$

The TD soft-decision symbols $\hat{\boldsymbol{x}}(k)$ are converted into FD signals $\hat{\boldsymbol{x}}(f) = [\hat{x}_1(f), \hat{x}_2(f), \ldots, \hat{x}_M(f)]^{\mathrm{T}} \in \mathbb{C}^{M\times 1}$. Subsequently, the soft-decision replicas in FD $\hat{\boldsymbol{y}}_m(f) \in \mathbb{C}^{L\times 1}$ are given by the following expression:

$$\hat{\boldsymbol{y}}_m(f) = \boldsymbol{h}_m(f)\hat{x}_m(f). \tag{5}$$

The soft cancellation and MMSE MIMO signal separation and equalization can be expressed as follows:

$$\tilde{x}_m(f) = \boldsymbol{w}_m^{\mathrm{H}}(f)\left(\boldsymbol{y}(f) - \sum_{i\neq m}\hat{\boldsymbol{y}}_i(f)\right), \tag{6}$$

$$\boldsymbol{w}_m(f) = \left(\boldsymbol{h}_m(f)\boldsymbol{h}_m^{\mathrm{H}}(f) + \sum_{i\neq m}\beta_i\boldsymbol{h}_i(f)\boldsymbol{h}_i^{\mathrm{H}}(f) + \sigma^2\mathbf{I}_L\right)^{-1}\boldsymbol{h}_m(f), \tag{7}$$

where $\boldsymbol{w}_m(f) \in \mathbb{C}^{L\times 1}$ is an MMSE filter with residual interference coefficients $\beta_m (0 \leq \beta_m \leq 1)$ as presented below [12], [14]:

$$\beta_m = \begin{cases} 0, & \text{Parity-check satisfied} \\ 1 - \dfrac{1}{K}\sum_k \left|\hat{x}_m(k)\right|^2, & \text{otherwise.} \end{cases} \tag{8}$$

Thus, β_m is set to 0 by satisfying all the parity-check equations of the mth stream based on hard decisions on *a posterior* LLRs. The coefficient β_m indicates the average residual symbol interference after cancellation [14].

The aforementioned processes, namely (4)–(8) and soft decoding, are repeated as the outer iteration.

B. EARLY STOPPING

Early stopping (ES) can reduce the computational complexity of iterative signal processing. In [15], it was revealed that the ES can improve the error performance in experimental performance evaluation. In this study, the residual interference coefficients given by (8) are exploited as a stopping metric. The outer iteration ended on satisfying the following inequality.

$$\sum_{m=1}^{M}\beta_m \leq \varepsilon. \tag{9}$$

The ε is an iteration control threshold. Therefore, ε can be adjusted to reduce the number of outer iterations, resulting in reduced computational complexity.

IV. ERROR-CONTROL SCHEME ON THE MS SIDE

A. RESIDUAL INTERFERENCE COEFFICIENTS BASED SELECTION SCHEME

In the proposed MS-side error-control scheme, the decision results of multiple detection MSs are used to improve detection performance. The residual interference coefficient (RIC) β_m is used as reliability information. Because this coefficient is inherent in FD iterative equalization, no increase in computational complexity is observed. The most reliable DBS is determined as the final bit sequence based on β_m. The error control on the MS side is performed on each stream independently.

The target MS checks its own residual interference coefficient, β_m. If β_m is larger than the threshold value β_0, the

target MS sends a request to other detection MSs. The request packet contains $\beta_m \forall m$ to avoid transferring a less reliable DBS. Specifically, the reliability metric of the mth stream in detection MSi is represented by $\beta_{i,m}$. When the detection MSi receives the request packet, the detection MSi transfers its own DBS to the target MS if $\beta_{i,m} < \beta_{h+1,m}$ holds, where MS$(h+1)$ is the target MS. The detailed process of this MS-side error-control scheme is described in Algorithm 1.

Algorithm 1 MS-Side Error-Control Scheme Based on Residual Interference Coefficients

Input: M: number of streams, $\beta_{i,m}$: β_m at the detection MSi, $S_{i,m}$: DBS of the mth stream at detection MSi,
Output: S_m: DBS of the mth stream
Initialization: $S_m = S_{h+1,m}\ \forall m$
for $m = 1$ to M **do**
  $i = h + 2$
  while $\beta_{h+1,m} > \beta_0$ **do**
    request $S_{i,m}$ and $\beta_{i,m}$ from the detection MSi
    if $\beta_{i,m} < \beta_{h+1,m}$ **then**
      detection MSi transfers $S_{i,m}$ and $\beta_{i,m}$ to the target MS.
      $S_m = S_{i,m}$
      $\beta_{h+1,m} = \beta_{i,m}$
    end if
    $i = i + 1$
  end while
end for
return $S_m\ \forall\ m$

V. COMPUTER SIMULATIONS

A. SYSTEM DESCRIPTION

The error ratio performance with the collaboration traffic volume was investigated through computer simulations. The BS employed four transmit antennas and transmitted $M = 4$ independent signal streams. The transmission packet is composed of a 39-symbol long orthogonal training sequence (TS) including a seven-symbol cyclic extension, four-symbol cyclic prefix (CP), and QPSK-modulated data sequence (DATA) of 192 symbols (low-density parity-check code, rate 1/2). The TSs are assigned to the signal streams in a deterministic but arbitrary manner.

In the collaborative group, we have six ($h + d = 6$) MSs, where several cases of h and d combinations are examined. The frame structure is displayed in Fig. 3. The M transmitted packets from the BS are received by the six MSs. The h helper MSs forwarded the received signals to the d detection MSs. The collaboration wireless links are supposed to be error free for simplicity because the transmission distance of the collaboration wireless links are assumed to be short. The threshold β_0 is assumed to be 0, while the channel matrices are estimated using the least square method. The numbers of outer and inner iterations were three and twelve, respectively.

B. SPATIAL CORRELATION

The effect of spatial correlation in the channel from the BS to the MSs on the error performance was studied. The transmit and receive correlation matrices $\boldsymbol{T} = \mathbb{E}[\boldsymbol{H}^{\mathrm{H}}\boldsymbol{H}]$ and $\boldsymbol{R} = \mathbb{E}[\boldsymbol{H}\boldsymbol{H}^{\mathrm{H}}]$ in the Kronecker model were formed according to

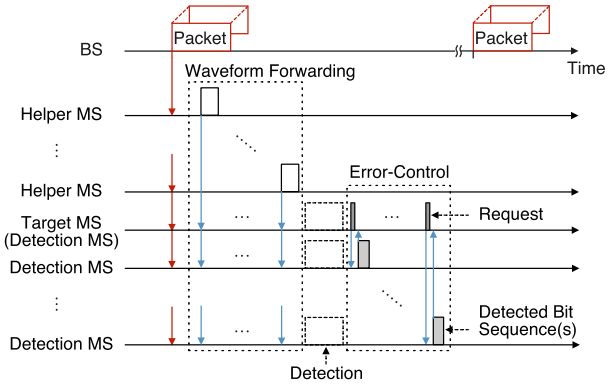

FIGURE 3. Frame structure of the MS-side error-control scheme. The helper MSs forward the packets received from the BS to the detection MSs. The detection MSs, except for the target MS, transmit their DBS(s) to the target MS upon request.

the exponential model of [16], where $\mathbb{E}[\cdot]$ is the expectation operator. The channel matrix with spatial correlation can be obtained as follows:

$$\boldsymbol{H} = \frac{1}{\sqrt{\kappa}}\boldsymbol{R}^{1/2}\boldsymbol{G}\left(\boldsymbol{T}^{1/2}\right)^{\mathrm{H}}, \tag{10}$$

where $\boldsymbol{G}$ is a pseudo-random $L \times M$ matrix whose elements follow an independently and identically distributed (i.i.d.) complex Gaussian process with zero mean and unit variance. The $\boldsymbol{R}^{1/2}$ and $\boldsymbol{T}^{1/2}$ are positive-semidefine matrices. κ is the trace of $\boldsymbol{R}$ and $\boldsymbol{T}$. The spatial correlation matrices are given by exponential correlation matrices,

$$\frac{[\boldsymbol{T}]_{i,j}}{N} = \frac{[\boldsymbol{R}]_{i,j}}{M} = \rho^{|i-j|}, \tag{11}$$

where $[\cdot]_{i,j}$ denotes the element in the ith row and the jth column of the matrix, and the parameter ρ is a real number ranging from 0 to 1.

C. TWO COMBINING SCHEMES FOR PERFORMANCE COMPARISON

The performance of the error-control scheme on the MS side with residual interference coefficients was compared with those of two combining schemes, namely an MC scheme [17] and an LLR combining scheme [18]. In the MC scheme, the target MS receives DBSs from other detection MSs, followed by a bit-by-bit majority combining using three DBSs. In the LLR combining scheme, the target MS receives LLR values of all bits from other detection MSs, and then hard decisions are made on the sum of the LLR values.

D. TRAFFIC OVER COLLABORATION LINKS

The traffic volume over the collaboration wireless links is measured in units of DBS (192 bits). The number of transferred DBS (TDBS) is incremented by one when a detection MS transfers a DBS of a single stream to the target MS. The traffic volume of waveform forwarding is measured in TDBS by assuming that the I and Q components of the received signal are quantized in eight bits each. Thus, forwarding a single received packet incurs 16 TDBS. Furthermore, a simple n-bit quantization is assumed to transfer the LLR values of a

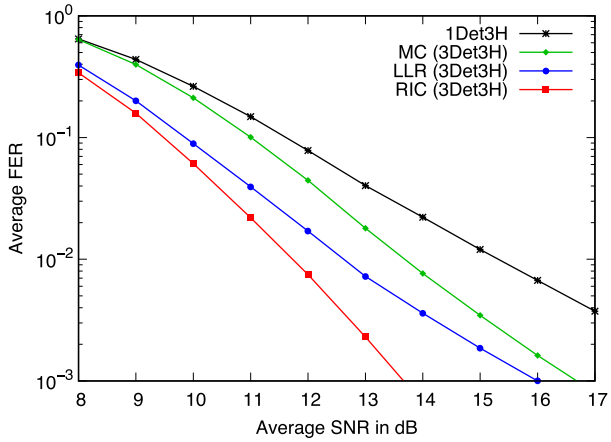

FIGURE 4. Average FER performance versus average SNR $\bar{\gamma}$ of MC, LLR, RIC over the frequency-flat fading channel. The number of helper MSs h is three. No quantization is applied for the LLR scheme.

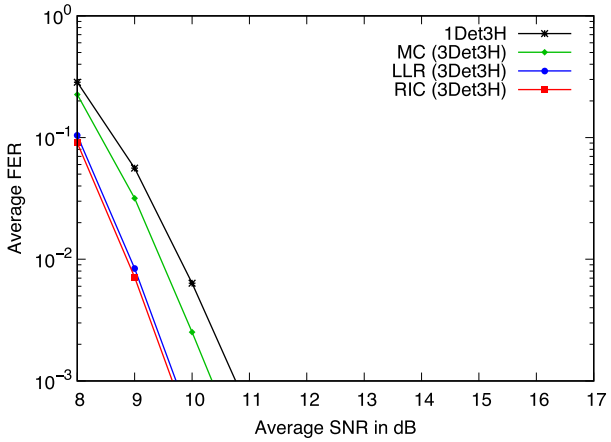

FIGURE 5. Average FER performance versus average SNR $\bar{\gamma}$ of MC, LLR, RIC over frequency-selective fading channel. The number of helper MSs h is three. No quantization is applied for the LLR scheme.

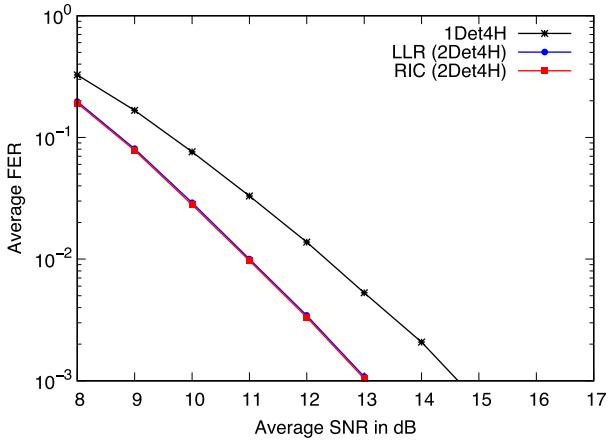

FIGURE 6. Average FER performance versus average SNR $\bar{\gamma}$ of MC, LLR, RIC over frequency-flat fading channel. The number of helper MSs h is four. No quantization is applied for the LLR scheme.

packet. Therefore, transferring LLR values of a single stream corresponds to n TDBS.

E. COMPUTER SIMULATION RESULTS

The system that consists of d detection MSs and h helper MSs is denoted as dDet$h$H. The normalized maximum Doppler frequency $f_{\mathrm{D}}T_{\mathrm{s}}$ was 6.4×10^{-5} throughout the computer simulations. Figs. 4 and 5 display the average FER performance of the proposed scheme in comparison with two combining schemes LLR and MC. The collaborative group included three detection MSs and three helper MSs (3Det3H, $d = 3, h = 3$).

The average FER performance as a function of the average signal-to-noise ratio (SNR) $\bar{\gamma}$ over frequency-flat i.i.d. Rayleigh fading channels is displayed in Fig. 4. The average FER performance of a single-detection MS scheme (1Det3H) is also displayed in this figure for comparison purposes. MS-side error control is not performed in 1Det3H because a single DBS is available for each stream. The average FER performance of the proposed RIC scheme was considerably improved compared with that of 1Det3H. This result revealed that the RIC scheme can select a superior DBS using the residual interference coefficients. The RIC scheme achieved a better average FER performance than the MC and LLR schemes.

The average FER performance over the frequency-selective channel is displayed in Fig. 5. As a channel model, a symbol-spaced four-tap i.i.d. Rayleigh fading with a flat power-delay profile is considered. The average FER performance of all schemes considerably improved because of the frequency diversity effects from FD MMSE equalization. The RIC scheme achieves the best FER performance in all schemes. These results reveal that the proposed RIC scheme outperformed the combining schemes in both frequency-flat and frequency-selective fading channels.

The average FER performance of the MS-side error-control schemes that included two detection MSs and four helper MSs (2Det4H) was studied. Fig. 6 illustrates the average FER performance over frequency-flat i.i.d. Rayleigh fading channels. Compared with Fig. 4, the average FER performances of 1Det4H and the LLR scheme were improved because the five received signals were used by FD MMSE equalization. The proposed RIC scheme outperformed 1Det4H scheme.

Identifying the performance degradation of a multiple-detector system in a spatially correlated channel is a critical consideration. The average FER performance over spatially correlated frequency-flat Rayleigh fading channels is presented in Fig. 7. The average SNR $\bar{\gamma}$ is 13 dB. This figure reveals the average FER performance of the RIC scheme, two combining schemes, and 1Det in both the $h = 3$ and $h = 4$ cases. The performance of the MC scheme is presented for the $h = 3$ case. As expected, spatial correlation exhibited a negative effect on the average FER performance in both cases. The average FER performance of the RIC scheme was superior to that of 1Det in both cases, even over spatially correlated channels.

Various combinations of d and h are displayed in Figs. 8 and 9. In Figs. 8 and 9, frequency-flat channels with $\bar{\gamma} = 12$ dB, and frequency-selective channels with $\bar{\gamma} = 8$ dB, respectively, were assumed. The vertical axis represents the

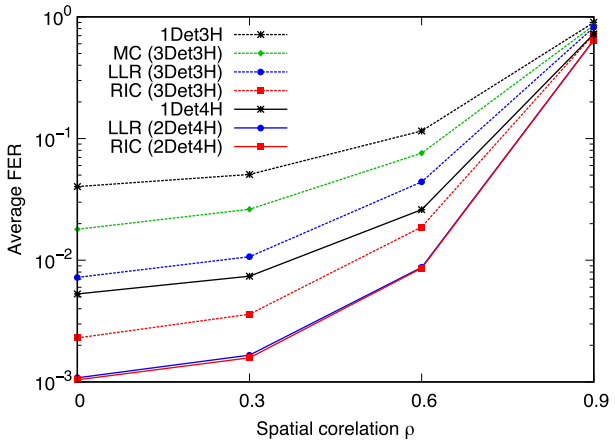

FIGURE 7. Average FER performance versus spatial correlation over frequency-flat fading channel with spatial correlation. The average SNR $\bar{\gamma}$ was 13 dB. No quantization is applied for the LLR scheme.

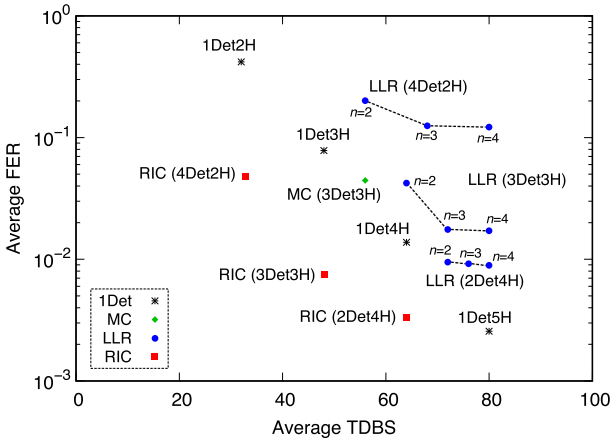

FIGURE 8. Average FER performance versus average TDBS over frequency-flat i.i.d. Rayleigh fading channels. The average SNR $\bar{\gamma}$ was 12 dB.

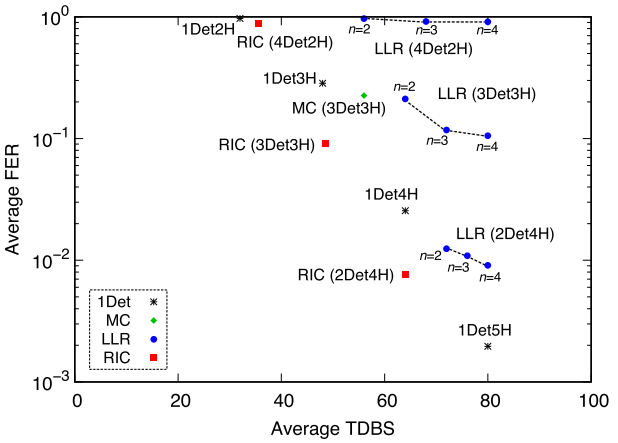

FIGURE 9. Average FER performance versus average TDBS over frequency-selective i.i.d. Rayleigh fading channels. The average SNR $\bar{\gamma}$ was 8 dB.

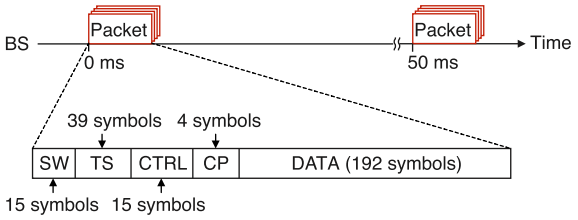

FIGURE 10. Frame structure of measurement campaign.

TABLE 1. Major parameters of the field measurements.

Parameter	Values
Carrier frequency	427.2 MHz
Symbol rate	312.5 ksps
Transmit power of BS	1 W
Number of BS antennas	4
Gain of BS antenna	5.8 dBi
BS antenna height	25.5 m
Cable loss	1.4 dB
Transmit filter	Square root raised cosine
	Roll-off factor 0.4
Frame interval	50 ms
Number of antennas of each MS	1
Number of MSs	6
Antenna of MS	$\lambda/4$ omnidirectional monopole
MS antenna height	2.1 m

average FER, and the horizontal axis represents the average TDBS. As observed in both figures, the proposed RIC scheme achieved superior or comparable FER performance to the LLR scheme with the same combination of d and h. The average TDBS of the RIC scheme is always less than that of the LLR scheme. The RIC scheme was superior to the 1Det scheme in terms of the average FER performance of the RIC and 1Det schemes for the same h, whereas the TDBSs were almost the same. The average FER performance and average TDBS of the MC scheme were between those of the 1Det and LLR schemes. Both figures included the performance of the 1Det scheme with five helpers (1Det5H) as a benchmark. 1Det5H performs the best in terms of the average FER performance at the expense of the increased traffic volume.

VI. FIELD EXPERIMENTS

A. EXPERIMENTAL SETUP

As displayed in Fig. 10, four packets are transmitted simultaneously from the BS to six MSs every 50 ms. The packet included a 15-symbol synchronization word for timing detection, an orthogonal TS, a 15-symbol control block (CTRL), 4-symbol CP, and a 192-symbol QPSK-modulated data block. The TS and DATA were the same as those used in computer simulation. The data bits were successively drawn from a pseudo-random sequence generator. The symbol rate was 312.5 kilo symbols per second (ksps) because of the bandwidth limitation of the radio license. The frequency and timing synchronizations were managed by 10 MHz signals and 1-pulse-per-second signals of global-positioning-system-based oscillators. The number of outer iterations was controlled by the ES, in which the iteration control threshold ε was 0.01. The noise variance was adjusted to provide the best performance. Table 1 reveals the major parameters of the field measurements.

The carrier frequency and transmission power were 427.2 MHz and 1 W per antenna, respectively. As displayed in Fig. 11, four BS antennas were located 25.5 m above the ground and placed in a 3.8 m × 2.5 m rectangle located on the rooftop of the building on the campus of Kyoto University.

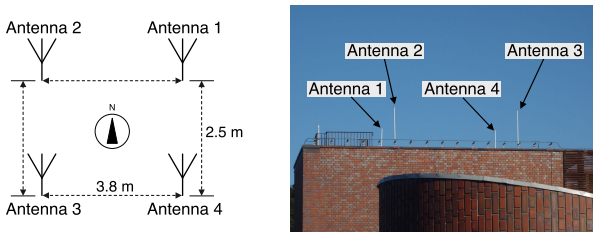

FIGURE 11. BS antennas are arranged in a rectangle on the top of a building.

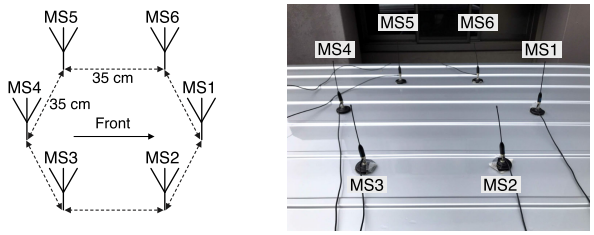

FIGURE 12. MS antennas mounted on the vehicle. The antennas are arranged in a uniform circular array.

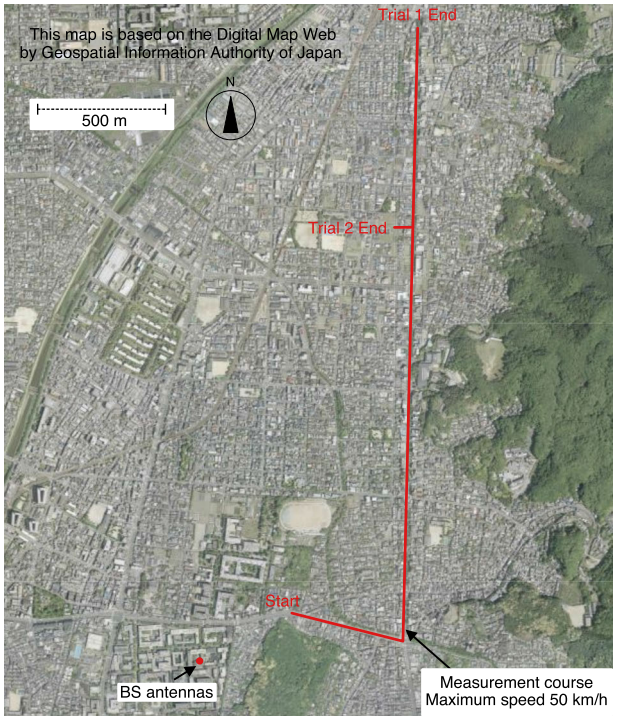

FIGURE 13. Location of the base station and route of the vehicle mounted with the antennas.

The BS antennas were 5.8 dBi omnidirectional in the horizontal plane. Six MS receive antennas were installed on the roof of the vehicle (2.1 m height), as displayed in Fig. 12. The receiving antennas were a $\lambda/4$ omnidirectional monopole antennas.

To record the received signals, the vehicle moved twice (i.e. trial 1 and 2) along the Imadegawa-dori and Shirakawa-dori streets in Kyoto city, as displayed in Fig. 13.

B. EXPERIMENTAL RESULTS

Fig. 14 illustrates the FER performance averaged over the trials 1 and 2. The horizontal axis is the average TDBS.

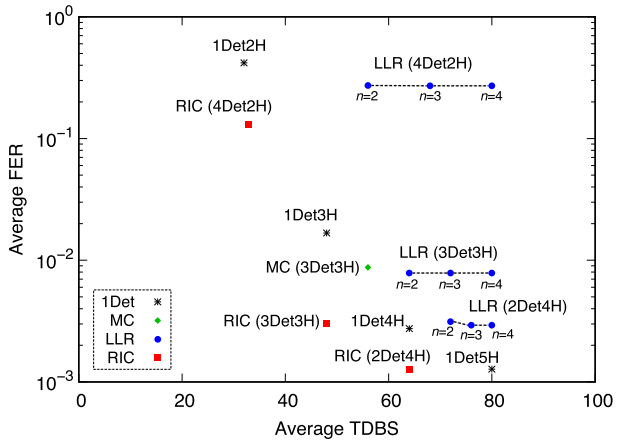

FIGURE 14. Average FER performance versus the average TDBS of four schemes with $h = 2, 3, 4, 5$. The results are averaged over two trials.

The number of helper MSs ranged from two to five because six MSs were considered in this measurement. The helper MSs and the detection MSs were selected in the numerical order; for example, MS1 and MS2 are helpers for the two-helper case, and MS1 through MS5 are helpers for the five-helper case. The detection MSs are the rest of the MSs.

As displayed in this figure, the RIC scheme achieved almost the best FER performance among all schemes with the same number of helper MSs h. Furthermore, comparing the RIC scheme and the 1Det scheme with the same number of h revealed that the average TDBS of the RIC scheme was marginally larger than that of the 1Det scheme. This increase in the average TDBS becomes negligible in the low FER region. In contrast to the previous results of the computer simulation, the 1Det5H scheme performance was almost the same as the RIC scheme of 2Det4H. The cause of this phenomenon requires further investigation.

VII. CONCLUSION

An MS-side error-control scheme that incorporates reliability metrics on a per-stream basis was proposed in this study. To demonstrate the effectiveness of the proposed scheme, the FER performance determined by computer simulations and field experiments were compared with those of two combining schemes. The proposed scheme can effectively improve FER performance by using residual interference coefficients to select better bit sequences. The proposed scheme that considers spatial correlation in fading channels exhibited a similar relationship between FER performance and spatial correlation. Furthermore, the proposed scheme suppressed the collaboration traffic volume by using multiple detection MSs, and the differences in the DBSs of multiple detection MSs are exploited with residual interference coefficients.

REFERENCES

[1] R. Dabora and S. D. Servetto, "Broadcast channels with cooperating decoders," *IEEE Trans. Inf. Theory*, vol. 52, no. 12, pp. 5438–5454, Dec. 2006.

[2] T. Okubo and M. Itami, "A study on cooperative reception of one segment ISDB-T," in *Proc. 2nd Int. Conf. Electr. Eng.*, Auckland, New Zealand, Jan. 2008, pp. 1–6.

[3] J. Hirosawa and T. Ohtsuki, "Collaborative decoding based on average LLR per segment," in *Proc. IEEE VTS Asia Pacific Wireless Commun. Symp. (APWCS)*, Sendai, Japan, Aug. 2008.
[4] A. Maaref, J. Ma, M. Salem, H. Baligh, and K. Zarin, "Device-centric radio access virtualization for 5G networks," in *Proc. IEEE Globecom Workshops (GC Wkshps)*, Austin, TX, USA, Dec. 2014, pp. 887–893.
[5] M. Dohler, J. Dominguez, and H. Aghvami, "Link capacity analysis for virtual antenna arrays," in *Proc. IEEE 56th Veh. Technol. Conf.*, Vancouver, BC, Canada, vol. 1, Sep. 2002, pp. 440–443.
[6] H. Murata, "Collaborative interference cancellation for multi-user MIMO communication systems," IEICE, Tokyo, Japan, Tech. Rep. RCS2013-201, Nov. 2013, vol. 113, no. 301, pp. 159–164.
[7] H. Murata and R. Shinohara, "Performance improvement of ZF-precoded MU-MIMO transmission by collaborative interference cancellation," *IEICE Commun. Exp.*, vol. 4, no. 5, pp. 155–160, 2015.
[8] H. Murata, R. Shinohara, and Y. Fujimoto, "Performance of adaptive mobile terminal selection schemes for collaborative MMSE linear MIMO detection," *IEICE Commun. Exp.*, vol. 8, no. 12, pp. 662–667, 2019.
[9] D. Fengning and H. Murata, "Performance study of terminal collaborated MIMO reception experimental testbed in actual environment," in *Proc. IEEE VTS Asia Pacific Wireless Commun. Symp. (APWCS)*, Singapore, Aug. 2019, pp. 1–5.
[10] F. Du, H. Murata, M. Kasai, T. Nakahira, K. Ishihara, M. Sasaki, and T. Moriyama, "Distributed detection of MIMO spatial multiplexed signals in terminal collaborated reception," *IEICE Trans. Commun.*, vol. 104, no. 7, pp. 884–892, 2020.
[11] H. Taromaru, H. Murata, T. Nakahira, M. Sasaki, and T. Moriyama, "Local ARQ: A new way for exploiting multiple detection-terminals," in *Proc. IEEE VTS 17th Asia Pacific Wireless Commun. Symp. (APWCS)*, Aug. 2021, pp. 1–4.
[12] T. Koike, H. Murata, and S. Yoshida, "Frequency-domain SC/MMSE iterative equalizer with MF approximation in LDPC-coded MIMO transmissions," in *Proc. IEEE 15th Int. Symp. Pers., Indoor Mobile Radio Commun.*, Sep. 2004, pp. 1414–1428.
[13] S. Minami, H. Nagano, and H. Murata, "Performance evaluation of iterative frequency domain equalization with LDPC code for user collaborated reception," IEICE, Tokyo, Japan, Tech. Rep. RCS2015-383, Mar. 2016, pp. 291–296.
[14] K. Kansanen and T. Matsumoto, "An analytical method for MMSE MIMO turbo equalizer EXIT chart computation," *IEEE Trans. Wireless Commun.*, vol. 6, no. 1, pp. 59–63, Jan. 2007.
[15] M. Kasai, H. Murata, T. Nakahira, K. Ishihara, and T. Moriyama, "Effect of early stopping on error performance of iterative MIMO equalization: An experience in reality," *IEICE Commun. Exp.*, vol. 9, no. 10, pp. 489–494, Oct. 2020.
[16] Y. Karasawa, "Channel capacity of massive MIMO with selected multi-stream transmission in spatially correlated fading environments," *IEEE Trans. Veh. Technol.*, vol. 69, no. 5, pp. 5320–5330, May 2020.
[17] V. Vukovic, G. Petrovic, and L. Trajkovic, "Packet error probability in a three-branch diversity system with majority combining," *IEEE Commun. Lett.*, vol. 15, no. 1, pp. 7–9, Jan. 2011.
[18] E. W. Jang, J. Lee, H.-L. Lou, and J. M. Cioffi, "On the combining schemes for MIMO systems with hybrid ARQ," *IEEE Trans. Wireless Commun.*, vol. 8, no. 2, pp. 836–842, Feb. 2009.

HOKUTO TAROMARU (Student Member, IEEE) received the B.E. degree from Ritsumeikan University, Shiga, Japan, in 2021. He is currently pursuing the M.E. degree with the Graduate School of Informatics, Kyoto University, Kyoto, Japan.

HIDEKAZU MURATA (Member, IEEE) received the B.E., M.E., and Ph.D. degrees in electronic engineering from Kyoto University, Kyoto, Japan, in 1991, 1993, and 2000, respectively.

In 1993, he joined the Faculty of Engineering, Kyoto University. From 2002 to 2006, he was an Associate Professor with the Tokyo Institute of Technology. He has been with Kyoto University, since October 2006, where he is currently an Associate Professor with the Department of Communications and Computer Engineering, Graduate School of Informatics. His research interests include signal processing and hardware implementation, particularly for application to cooperative wireless networks.

Prof. Murata received the Young Researcher's Award from IEICE of Japan, in 1997; the Ericsson Young Scientist Award, in 2000; the Young Scientists' Prize of the Commendation for Science and Technology by the Minister of Education, Culture, Sports, Science and Technology, in 2006; the Best Paper Award of IEICE, in 2011 and 2013; and the IEEE ICC Best Paper Award, in 2014. He is a member of IEICE and ITE.

TOSHIRO NAKAHIRA received the bachelor's degree in maritime safety from the Japan Coast Guard Academy, in 2009, and the M.I. degree in informatics from Kyoto University, in 2012. In 2012, he joined the NTT Network Innovation Laboratories. He is currently working with the NTT Access Network Service Systems Laboratories. His research interests include natural area design and dynamic control techniques using multiple wireless access. He is a member of IEICE. He received the Best Research Award of the Fourth Basic Course Workshop of the Institute of Electronics, Information and Communication Engineers (IEICE) Communication Quality, in 2017, and the Young Engineer Award from IEICE, in 2019.

DAISUKE MURAYAMA (Member, IEEE) received the B.E., M.E., and Ph.D. degrees in electrical engineering from Keio University, Kanagawa, Japan, in 2005, 2007, and 2015, respectively. Since 2007, he has been with the NTT Access Network Service Systems Laboratories, NTT Corporation, Kanagawa, where he works on wireless and optical access networks and systems. His current research interests include 5G NR and other unlicensed wireless access networks, passive optical networks, system control, and measurement engineering. He is a member of IEICE.

TAKATSUNE MORIYAMA received the B.E. and M.E. degrees from the Muroran Institute of Technology, Japan, in 1991 and 1993, respectively. He joined NTT, in 1993. Since 1999, he has been working with the NTT Communications, where he led network service development and operations for corporate customers. He has been in his current position, since July 2019.